Energy-pooling collisions in Rb-Cs vapor mixture $Rb(5P_J)+Cs(6P_{3/2}) \rightarrow Rb(5S_{1/2})+Cs(nl_{J'})$

Yifan Shen (沈异凡), Kang Dai (戴 康), Baoxia Mu (穆保霞), Shuying Wang (王淑英), and Xiuhua Cui (崔秀花)

Department of Physics, Xinjiang University, Urumqi 830046

Received May 9, 2006

Rate coefficients for energy-pooling (EP) collisions $Rb(5P_J) + Cs(6P_{3/2}) \rightarrow Rb(5S_{1/2}) + Cs(nl_{J'})$ have been measured. Atoms were excited to $Rb(5P_J)$ and $Cs(6P_{3/2})$ states using two single-mode diode lasers. To isolate the heteronuclear contribution in the fluorescence spectrum, a double-modulation technique has been adopted. The excited-atom density and spatial distribution are mapped by monitoring the absorption of a counterpropagating single-mode diode laser beam, tuned to $Rb(5P_J \rightarrow 7S_{1/2})$ and $Cs(6P_{3/2} \rightarrow 8S_{1/2})$ transitions respectively, which could be translated parallelly to the pump beams. The excited atom densities are combined with the measured fluorescence ratios to determine cross sections for the EP processes. It was found that $Rb(5P_{1/2})+Cs(6P_{3/2})$ collisions are more efficient than $Rb(5P_{3/2})+Cs(6P_{3/2})$ collisions for populating $Cs(4F_{5/2})$, while the opposite is true for populating $Cs(4F_{7/2})$.

OCIS codes: 020.0020, 020.2070, 020.3690.

In energy-pooling (EP) collisions[1−5] two excited atoms produce one ground-state and one very-excited-state atom under the condition that the total internal energy is preserved in the limit of kT. Therefore the energy of the final excited level must be $E = E_1 + E_2 + \Delta E$, where E_1 and E_2 are the energies of the two laser-populated levels and $\Delta E \approx kT$. This condition imposes severe limitations on the number of possible EP resonances for a given atom. The simultaneous excitation of atoms of two different species in a vapor mixture increases the number of possible "quasi" resonances and it proposes new interesting level scheme combinations. Moreover, it opens the possibility of the theoretical and experimental studies on the interatomic potentials between different atoms in an important range of interatomic distance.

Namiotka *et al.*[2] reported experimental rate coefficients for EP process $K(4P_J)+K(4P_J) \rightarrow K(4S)+K(nl)$ with product states $nl = 5P$, $6S$, and $4D$, and found that the angular momentum propensity rules can play a role in the EP processes.

Here we report the results of an experimental investigation of EP processes

$$Rb(5P_J) + Cs(6P_{3/2}) \rightarrow Rb(5S) + Cs(8S, 4F). \quad (1)$$

The $Rb(5P_J)$ fine-structure splitting is large enough to allow a separate study of the $Rb(5P_{1/2}) + Cs(6P_{3/2})$ and $Rb(5P_{3/2}) + Cs(6P_{3/2})$ collision processes. Thus the study of angular momentum in the EP processes is independent of energy deficits (see Fig. 1).

It is evident that the double resonant excitation produces a very rich spectra. These spectra are more crowded because of the separate contributions of the homonuclear and of the heteronuclear collisions. In order to measure the heteronuclear rate constants of reaction (1) it is therefore necessary to isolate the signal of reaction (1) from all the others.

We have solved the problem by adopting an intermodulation technique that can be used every time heteronuclear processes take place. The two laser beams are modulated at two different frequencies ω_1 and ω_2, and the fluorescence is phase detected at $\omega_1+\omega_2$. This procedure filters out the homonuclear part of the spectrum, which will have only one of the two modulation frequencies, and it transmits the heteronuclear contribution, which will have components modulated at the sum frequency.

By assuming that other processes, such as multiphoton excitation, atomic ionization etc., are negligible (the experimental conditions are chosen to minimize them). For pumping $Rb(5P_J)$ and $Cs(6P_{3/2})$ states, the steady state rate equations for reaction (1) is

$$[Cs_{nl_{J'}}(\vec{r})] = k_{nl_{J'}} \tau^e_{nl_{J'}} [Rb_{5P_J}(\vec{r})][Cs_{6P_{3/2}}(\vec{r})], \quad (2)$$

where $k_{nl_{J'}}$ is the EP rate coefficient, $[Cs_{nl_{J'}}(\vec{r})]$, $[Rb_{5P_J}(\vec{r})]$, and $[Cs_{6P_{3/2}}(\vec{r})]$ are the densities in atomic levels $Cs\,(nl_{J'})$, $Rb(5P_J)$, and $Cs(6P_{3/2})$, respectively, $\tau^e_{nl_{J'}}$ is the effective lifetime for atoms in the states $Cs\,(nl_{J'})$. However, in the present case, the trapping on all transitions of interest is negligible (i.e., $\tau^e_{nl_{J'}} = \tau_{nl_{J'}}$). Note that in the absence of quenching collisions and

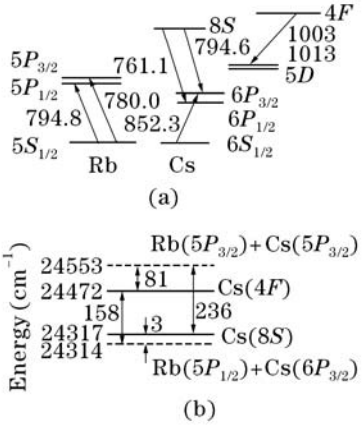

Fig. 1. (a) Energy levels of rubidium and cesium transitions. Wavelengths are given in nanometer; (b) Cesium atomic levels lying near the $Rb(5P_J) + Cs(6P_{3/2})$ energies (dashed lines).

radiation trapping, $[\tau_{nl_{J'}}]^{-1}$ is just the sum of the Einstein A coefficients for transitions connecting state $nl_{J'}$ to all lower levels.

Under the low density of ground-state atoms, a complete model for cesium EP collisions has been presented in Ref. [1], in which the EP rate coefficient in terms of the measured fluorescence ratios is given. EP collisions (reaction (1)) can be treated analogously and so here we only quote the result

$$k_{nl_{J'}} = \frac{I_{nl_{J'}\to n'l'_{J''}}/\varepsilon_{nl_{J'}\to n'l'_{J''}}}{I_{6P_{3/2}\to 6S_{1/2}}/\varepsilon_{6P_{3/2}\to 6S_{1/2}}} \cdot \frac{\lambda_{nl_{J'}\to n'l'_{J''}}}{\lambda_{6P_{3/2}\to 6S_{1/2}}} \times \frac{\Gamma^n_{6P_{3/2}\to 6S_{1/2}} T_{6P_{3/2}\to 6S_{1/2}}}{\Gamma^n_{nl_{J'}\to n'l'_{J''}} T_{nl_{J'}\to n'l'_{J''}}} \times \frac{1}{\tau^e_{nl_{J'}}} \frac{\int_{-R}^{R}[\mathrm{Cs}_{6P_{3/2}}(x)]\mathrm{d}x}{\int_{-R}^{R}[\mathrm{Rb}_{5P_J}(x)][\mathrm{Cs}_{6P_{3/2}}(x)]\mathrm{d}x}, \quad (3)$$

where $I_{nl_{J'}\to n'l'_{J''}}$ is the fluorescence intensity corresponding to the transition $nl_{J'} \to n'l'_{J''}$, $\varepsilon_{nl_{J'}\to n'l'_{J''}}$ the detection system efficiency (including effects due to the photomultiplier, monochromator grating, and any lens used) at the frequency of interest, and $\lambda_{nl_{J'}\to n'l'_{J''}}$ the transition wavelength; R is the radius; Γ^n is the natural radiative rate; T is the average probability that a photon emitted in the detection direction passes through the vapor between its point of origin and the cell walls without being absorbed. It is related to the frequency-dependent absorption cross section (including hyperfine structure), the density, and spatial distribution of atoms in the lower level transition, and is given explicitly in Eqs. (8)—(11) of Ref. [1]. We note that in the experiment, T is approximately equal to 1 except for the $6P_{2/3} \to 6S_{1/2}$ resonance transition. The resonance broadening rates of Ref. [6] were used to calculate the $T_{6P_{2/3}\to 6S_{1/2}}$. Experimentally, the measured quantities are $I_{nl_{J'}\to n'l'_{J''}}$, $\varepsilon_{nl_{J'}\to n'l'_{J''}}$, $I_{6P_{3/2}\to 6S_{1/2}}$, $\varepsilon_{6P_{3/2}\to 6S_{1/2}}$, $[\mathrm{Rb}_{5P_J}(x)]$, and $[\mathrm{Cs}_{6P_{3/2}}(x)]$.

Figure 2 shows the set-up of the experiment. A Rb-Cs alloy was confined in a cylindrical cell with the inner diameter of 1.2 cm and the length of 6 cm. The cell was sealed after baking and evacuating until a vacuum of 10^{-4} Pa was reached. The alloy in the cell consisted of 70% rubidium and 30% cesium, and provided approximately equal atom densities according to Raoult's law. The cell was placed inside an oven. The temperatures of the cell ranging from 337 to 347 K were measured with thermocouples. The total density in the cell is of the order of 10^{11} cm^{-3}. This procedure gives reasonably comparable vapor pressures and avoids the problems connected to secondary processes induced by too high vapor pressure of one of the two elements.

Two lasers (Toptica DL100, linewidth of $\sim$ 1 MHz) were used to excite rubidium (laser1) and cesium (laser2) respectively. Laser1 was a single mode diode laser with a maximum output power of 40 mW, laser2 is also a single mode diode laser with 70 mW. The wavelengths were 794.8 (or 780.0) and 852.3 nm. A chopper modulated the two beams at the frequencies ω_1 and ω_2. The lock-in

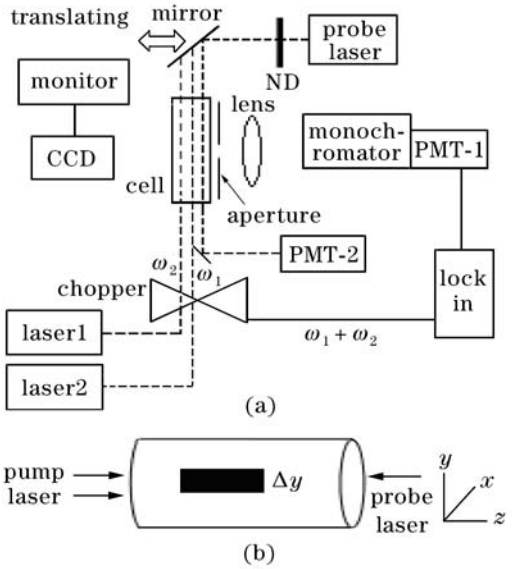

Fig. 2. (a) Experimental setup; (b) Inset showing the cell geometry and the region (shaded) from which fluorescence was detected.

amplifier (stanford research system SR830) was tuned to the sum frequency. The resonance fluorescence signals were observed with an infrared sensitive charge coupled device (CCD) camera during the alignment of the laser beams along the cell axis. We tuned the laser frequencies to maximize $\mathrm{Rb}(5P_J \to 5S_{1/2})$ and $\mathrm{Cs}(6P_{3/2} \to 6S_{1/2})$ fluorescence from the observation region. At the lower densities, the attenuation of the laser beams along the cell length could generally be neglected even when the laser was tuned directly to resonance.

A pair of lenses was used to image fluorescence onto the slits of 0.66-m monochromator (Acton AM566) with 1200-groove/mm grating. With 300 μm-slits (providing a spectral resolution of $\sim$ 0.6 nm) the volume from which fluorescence was collected was a strip with the width of $\sim$ 0.5 mm and the length of 5 mm along the lasers propagation axis (z-direction). A photomultiplier tube (PTM-1) was used to detect the resolved fluorescences $\mathrm{Cs}(6P_{3/2} \to 6S_{1/2})$ and $\mathrm{Cs}(nl_{J'} \to n'l'_{J''})$. The wavelength-dependent relative detection-system efficiency was measured using a calibrated tungsten-halogen lamp.

A single-mode diode laser was used to probe the density and spatial distributions of the atoms in $\mathrm{Rb}(5P_{1/2})$ level. The power of the probe laser was cut down to $\sim$ 1 μW with neutral density filters. We directly measure the $5P_{1/2}$ density by scanning the probe laser over the $\mathrm{Rb}(5P_{1/2} \to 7S_{1/2})$ transition and monitoring its transmission using another photomultiplier tube (PMT-2). In order to measure the spatial dependence $[\mathrm{Rb}_{5P_{1/2}}(x)]$ across the diameter of the cell, the probe laser was stepped across the cell parallel to the pump beam using the translating mirror as shown in Fig. 2.

The transmitted intensity of the probe laser beam through a length L of the vapor is given by

$$I_\nu = I_\nu(0)\mathrm{e}^{-k_{7S_{1/2}\leftarrow 5P_{1/2}}(\nu)L} \quad (4)$$

for the light of frequency ν. Here $I_\nu(0)$ is the incident intensity and $k_{7S_{1/2}\leftarrow 5P_{1/2}}$ is the frequency-dependent

Table 1. Rate Coefficients for the EP Collisions Rb($5P_J$)+Cs($6P_{3/2}$) → Rb($5S$)+Cs($nl_{J'}$)

$nl_{J'}$	T (°C)	$n_{6S_{1/2}}$ (10^{11} cm^{-3})	Ratio 1	Monitored Transion $nl_{J'} \rightarrow n'l'_{J''}$	Ratio 2	$\gamma_{nl_{J'}\rightarrow n'l'_{J''}}$	$\Gamma^e_{6P_{3/2}\rightarrow 6S_{1/2}}$ (s^{-1})	$k_{nl_{J'}}$ (cm^{3}s^{-1})
$\mathrm{Rb}\left(5P_{1/2}\right)+\mathrm{Cs}\left(6P_{3/2}\right)\rightarrow \mathrm{Rb}\left(5S\right)+\mathrm{Cs}\left(nl_{J'}\right)$ $(J=1/2)$								
$4F_{5/2}$	64	2.72	$(1.41\times10^9)^{-1}$	$4F_{5/2}\rightarrow 5D_{3/2}$	6.10×10^{-8}	0.877	4.53×10^6	2.64×10^{-10}
	74	5.70	$(3.79\times10^9)^{-1}$		3.92×10^{-7}		1.94×10^6	2.71×10^{-10}
$4F_{7/2}$	64	2.72	$(1.41\times10^9)^{-1}$	$4F_{7/2}\rightarrow 5D_{5/2}$	3.30×10^{-8}	0.936	4.53×10^6	1.35×10^{-10}
	74	5.70	$(3.79\times10^9)^{-1}$		2.16×10^{-7}		1.94×10^6	1.41×10^{-10}
$8S_{1/2}$	64	2.72	$(1.41\times10^9)^{-1}$	$8S_{1/2}\rightarrow 6P_{3/2}$	1.93×10^{-7}	0.380	4.53×10^6	15.2×10^{-10}
	74	5.70	$(3.79\times10^9)^{-1}$		1.08×10^{-6}		1.94×10^6	13.5×10^{-10}
$\mathrm{Rb}\left(5P_{3/2}\right)+\mathrm{Cs}\left(6P_{3/2}\right)\rightarrow \mathrm{Rb}\left(5S\right)+\mathrm{Cs}\left(nl_{J'}\right)$ $(J=3/2)$								
$4F_{5/2}$	64	2.72	$(2.15\times10^9)^{-1}$	$4F_{5/2}\rightarrow 5D_{3/2}$	1.29×10^{-7}	0.877	4.53×10^6	3.65×10^{-10}
	74	5.70	$(5.87\times10^9)^{-1}$		9.03×10^{-7}		1.94×10^6	4.01×10^{-10}
$4F_{7/2}$	64	2.72	$(2.15\times10^9)^{-1}$	$4F_{7/2}\rightarrow 5D_{5/2}$	2.79×10^{-7}	0.936	4.53×10^6	7.45×10^{-10}
	74	5.70	$(5.87\times10^9)^{-1}$		1.97×10^{-6}		1.94×10^6	8.28×10^{-10}
$8S_{1/2}$	64	2.72	$(2.15\times10^9)^{-1}$	$8S_{1/2}\rightarrow 6P_{3/2}$	1.63×10^{-8}	0.380	4.53×10^6	8.42×10^{-11}
	74	5.70	$(5.87\times10^9)^{-1}$		9.03×10^{-8}		1.94×10^6	7.32×10^{-11}

Ratio 1: $\frac{\int_{-R}^{R}\left[\mathrm{Cs}\left(6P_{3/2}(x)\right)\right]\mathrm{d}x}{\int_{-R}^{R}\left[\mathrm{Rb}(5P_J)\right]\left[\mathrm{Cs}\left(6P_{3/2}\right)\right]\mathrm{d}x}$; Ratio 2: $\frac{I_{nl_{J'}\rightarrow n'l'_{J''}}/\varepsilon_{nl_{J'}\rightarrow n'l'_{J''}}}{I_{6P_{3/2}\rightarrow 6S_{1/2}}/\varepsilon_{6P_{3/2}\rightarrow 6S_{1/2}}}$; $\gamma_{nl_{J'}\rightarrow n'l'_{J''}}=\Gamma_{nl_{J'}\rightarrow n'l'_{J''}}\times\tau_{nl_{J'}}$; $\Gamma^e_{6P_{3/2}\rightarrow 6S_{1/2}}=\Gamma^n_{6P_{3/2}\rightarrow 6S_{1/2}}T_{6P_{3/2}\rightarrow 6S_{1/2}}$, $\Gamma^n_{6P_{3/2}\rightarrow 6S_{1/2}}=3.26\times10^7$ s^{-1}.

absorption coefficient. $[\mathrm{Rb}_{5P_{1/2}}]$ is related to the integral of $k_{7S_{1/2}\leftarrow 5P_{1/2}}$ by

$$\int k_{7S_{1/2}\leftarrow 5P_{1/2}}(\nu)\mathrm{d}\nu=\frac{(\lambda_{7S_{1/2}\leftarrow 5P_{1/2}})^2}{8\pi}\times\frac{g_{7S_{1/2}}}{g_{5P_{1/2}}}[\mathrm{Rb}_{5P_{1/2}}]\Gamma_{7S_{1/2}\leftarrow 5P_{1/2}},\qquad(5)$$

where $g_{7S_{1/2}}$ and $g_{5P_{1/2}}$ are the degeneracies of the $7S_{1/2}$ and $5P_{1/2}$ states, respectively. Thus we can extract $[\mathrm{Rb}_{5P_{1/2}}(x)]$ from the position-dependent probe transmission scans using Eqs. (4) and (5). Then the probe laser was tuned to $\mathrm{Rb}(5P_{3/2}\rightarrow 7S_{1/2})$ or $\mathrm{Cs}(6P_{3/2}\rightarrow 8S_{1/2})$ transition. The $\left[\mathrm{Rb}_{5P_{3/2}}(x)\right]$ and $[\mathrm{Cs}_{6P_{3/2}}(x)]$ can also be obtained analogously.

The measurement procedures are listed as follows. a) The two lasers were switched on and a spectrum with heteronuclear EP signal was recorded; b) the rubidium resonant laser (laser1) switched off and the lock-in amplifier was tuned to frequency ω_2, the fluorescence of transition $6P_{3/2}\rightarrow 6S_{1/2}$ was measured; c) the pump beams were not chopped; the probe laser frequency was tuned to $\mathrm{Rb}(5P_J\rightarrow 7S_{1/2})$ or $\mathrm{Cs}(6P_{3/2}\rightarrow 8S_{1/2})$ transition and absorption of the probe intensity was monitored; d) the line intensities were corrected according to the instrument response.

Position-dependent $\mathrm{Rb}(5P_J)$ state and $\mathrm{Cs}(6P_{3/2})$ densities were numerically integrated over the observation zone (cell diameter) to yield the factors $\int_{-R}^{R}[\mathrm{Cs}_{6P_{3/2}}(x)]\mathrm{d}x/\int_{-R}^{R}[\mathrm{Rb}_{5P_J}(x)][\mathrm{Cs}_{6P_{3/2}}(x)]\mathrm{d}x$ in Eq. (3) and then combined with the measured fluorescence ratios (corrected for detecting system efficiency) to yield the EP rate coefficients. The rate coefficient values obtained at different temperatures are given in Table 1.

An estimate of the statistical errors in the measured rate coefficients can be obtained by Eq. (3). Fluorescence ratios probably have an uncertainty as much as 25% because the $nl_{J'}\rightarrow n'l'_{J''}$ fluorescence signals were weak. We estimate the uncertainties in the ratio $\int_{-R}^{R}[\mathrm{Cs}_{6P_{3/2}}(x)]\mathrm{d}x/\int_{-R}^{R}[\mathrm{Rb}_{5P_J}(x)][\mathrm{Cs}_{6P_{3/2}}(x)]\mathrm{d}x$ to be approximately 15%. Value of $\tau_{nl_{J'}}$[7] is probably good to within 10%, while the values of $\Gamma_{nl_{J'}\rightarrow n'l'_{J''}}$ are accurate to at least 10% because the trapping is much less severely on this transition. $\Gamma^e_{6P_{3/2}\rightarrow 6S_{1/2}}$ may be uncertain by as much as 30%[1]. We estimate overall errors of $\sim 45\%$ in the measured EP rate coefficients.

Using the mean thermal velocity

$$\overline{v}=\left(\frac{8RT}{\pi}\cdot\frac{M_1+M_2}{M_1M_2}\right)^{1/2}=2.01\times10^3\ \mathrm{T}^{1/2}\mathrm{cm}\cdot\mathrm{s}^{-1}.\qquad(6)$$

We can calculate an average cross sections defined by $\sigma_{nl_{J'}}=k_{nl_{J'}}/\overline{v}$. The results are listed in Table 2.

Table 2. EP Rate Coefficients and Cross Sections for Rb($5P_J$)+Cs($6P_{3/2}$) → Rb($5S$)+Cs($nl_{J'}$)

J	$nl_{J'}$	Rate Coefficients (cm$^3\cdot$s^{-1})	Cross Sections (cm^2)
1/2	$4F_{5/2}$	$(2.7\pm1.2)\times10^{-10}$	$(7.2\pm3.2)\times10^{-15}$
	$4F_{7/2}$	$(1.4\pm0.6)\times10^{-10}$	$(3.8\pm1.7)\times10^{-15}$
	$8S_{1/2}$	$(14\pm6)\times10^{-10}$	$(3.8\pm1.7)\times10^{-14}$
3/2	$4F_{5/2}$	$(3.8\pm1.7)\times10^{-10}$	$(10.2\pm4.6)\times10^{-15}$
	$4F_{7/2}$	$(7.9\pm3.6)\times10^{-10}$	$(21.1\pm9.6)\times10^{-15}$
	$8S_{1/2}$	$(7.9\pm3.6)\times10^{-11}$	$(2.1\pm1.0)\times10^{-15}$

The results of Table 2 show that Cs($8S$) state is more effectively populated by Rb($5P_{1/2}$) + Cs($6P_{3/2}$) collisions than by Rb($5P_{3/2}$) + Cs($6P_{3/2}$) collisions. This can be explained strictly on the basis of energy deficits. Rb($5P_{1/2}$)+Cs($6P_{3/2}$) is more resonant than Rb($5P_{3/2}$)+ Cs($6P_{3/2}$) with Cs($8S$) (see Fig. 1(b)). For the Cs($4F$) levels we find that Cs($4F_{5/2}$) level is more strongly populated than Cs($4F_{7/2}$) by Rb($5P_{1/2}$)+Cs($6P_{3/2}$) collisions while $4F_{7/2}$ is more strongly populated than $4F_{5/2}$ by Rb($5P_{3/2}$)+Cs($6P_{3/2}$) collisions. Thus the differences between Rb($5P_{1/2}$)+Cs($6P_{3/2}$) and Rb($5P_{3/2}$)+Cs($6P_{3/2}$) collisions may indicate that angular momentum propensity rules can play a role in the EP process.

This work was partially supported by the National Natural Science Foundation of China under Grant No. 10264004. Y. Shen's e-mail address is shenyifan01 @xju.edn.cn.

References

1. Z. J. Jabbour, R. K. Namiotka, J. Huennekens, M. Allegrini, S. Milošević, and F. de Tomasi, Phys. Rev. A **54,** 1372 (1996).
2. R. K. Namiotka, J. Huennekens, and M. Allegrini, Phys. Rev. A **56,** 514 (1997).
3. Y.-F. Shen, K. Dai, B.-X. Mu, S.-Y. Wang, and X.-H. Cui, Chin. Phys. Lett. **22,** 2805 (2005).
4. C. Gabbanini, S. Gozzini, G. Squadrito, M. Allegrini, and L. Moi, Phys. Rev. A **39,** 6148 (1989).
5. Y. Shen and K. Dai, Chin. J. Lasers (in Chinese) **31,** (Suppl.) 17 (2004).
6. Z. J. Jabbour, J. Sagle, R. K. Namiotka, and J. Huennekens, J. Quantum Spectrosc. Radiat. Transfer **54,** 767 (1995).
7. C. E. Theodosiou, Phys. Rev. A **30,** 2881 (1984).